

## Unsynchronized and synchronized vertical migration of zooplankton in a high arctic fjord

*Finlo R. Cottier*

Scottish Association for Marine Science, Dunstaffnage Marine Laboratory, Oban, Argyll, PA37 1QA, United Kingdom

*Geraint A. Tarling*

British Antarctic Survey, Natural Environment Research Council, High Cross, Madingley Road, Cambridge, CB3 0ET, United Kingdom

*Anette Wold and Stig Falk-Petersen*

Norwegian Polar Institute, Polar Environment Research Centre, N-9296 Tromsø, Norway

1

### Abstract

We measured vertical migration of zooplankton in an arctic fjord at 79°N between June and September 2002 and transcending a period of continuous illumination to one of true day and night to investigate the changing influence of light cues on behavior. Observations made with a moored 300 kHz acoustic Doppler current profiler indicated that two modes of vertical migration occurred during the study period. During the weeks of continuous illumination, backscatter data indicated that there was no net vertical displacement of the population at any time during the 24-h period, but vertical velocity showed a continuous net downward movement in the surface layers and a net upward movement at depth. We interpreted this as unsynchronized vertical migrations by individuals with upward trajectories that slowed closer to the surface and downward trajectories that were most rapid in their initial phases. Synchronized migrations, seen as an upward and downward movement of scattering layers at dusk and dawn respectively, began once true nighttime resumed toward autumn. It is likely that the relative rate of change in light was used as the proximal cue for synchronized migrations. Concurrent net samples identified *Calanus finmarchicus* and *C. glacialis* as the most likely contributors to the unsynchronized migration patterns. The high backscatter of the synchronized scattering layers suggests that they included additional taxa such as the euphausiid *Thysanoessa* spp., the pteropod *Limacina helicina*, or the hyperiid amphipod *Themisto* spp.

The vertical migration of zooplankton between upper and deeper layers is common to all marine and freshwater environments (Ringelberg 1995). It is generally accepted that the behavior maximizes the evolutionary fitness of these organisms through satisfying the need to feed while minimizing exposure to visual predation (Gliwicz 1986). Although a variety of vertical migration patterns exists (Hays et al. 2001), the most common involves individuals moving to the surface layers during nighttime and descending to depth during the day. This results in the zooplankton entering the food-rich surface layers when the

detection capabilities of their visual predators are at their lowest. Many organisms use external cues to coordinate their vertical migrations with this daily change in circumstances. Many cues have been identified, but the vast majority are based around certain features of the light cycle, primarily the rate of change at a certain depth (Fortier et al. 2001) or the changing position of an isolume (Frank and Widder 1997). In effect, the reasons for undertaking a vertical migration (ultimate causes) are often difficult to separate from the mechanisms used to coordinate it (proximate causes) because changing light levels are instrumental to both. This makes it difficult for field studies to determine what is driving the vertical migration behavior and how flexible the patterns are.

During early and midsummer at high latitudes, when the sun does not set, relative light levels do not change rapidly within the daily cycle—a characteristic that sets true polar environments apart from other regions. In the marine context, this has the largest impact on the arctic, where open-water zooplankton communities can be found beyond latitudes of 80°N (in the Southern Hemisphere, this extreme poleward extent is limited by the continental land mass of Antarctica). At such high latitudes, the sun may not set for up to 4 months in the year. There is no optimal time for zooplankton to visit the surface layers during this summer period because the continuous illumination maintains the threat from visual predation. Further, the relative rate of change of illumination is minimal at this time, such

### Acknowledgments

We thank C. Griffiths, M. Inall, and P. Provost of SAMS and F. Nilsen of UNIS for support with the mooring operations, the masters, crews, and PSOs of the many research cruises that contributed to the mooring and CTD operations, and the Alfred Wegener Institute for access to irradiance data from Koldewey Station. The majority of this work was funded by UK Natural Environment Research Council through SAMS Northern Seas Program; European LSF grant NP-62/2002; and Norwegian Research Council as a part of the “On Thin Ice” research project. We benefited greatly in the production of this paper through funding from the Royal Society through a European Joint Project grant. The contribution of G.T. was carried out as part of the FLEXICON project of the DISCOVERY 2010 program at BAS. We thank the three reviewers for their encouraging and insightful comments.

that its efficacy as a cue to coordinate vertical migration (e.g., Tarling et al. 2002) may be reduced. In this instance, the ultimate causes of migration may become separated from the light-mediated proximal cues that coordinate it. Most zooplankton studies in this environment have failed to find any coordinated vertical migration during summer (Fischer and Visbeck 1993; Dale and Kaartvedt 2000; Blachowiak-Samolyk et al. 2006 and references therein) with individuals distributed through the water column and little apparent significant change in their depth over daily cycles. Coordinated vertical migrations then resume toward autumn, when the sun starts to set and true darkness occurs (Fischer and Visbeck 1993).

The conclusion that individuals do not vary their vertical position under continuous light conditions can be rationalized if food was available throughout the water column. However, this is not the case in most arctic environments because phytoplankton, the main food of many of the arctic zooplankton species, declines rapidly with depth (Fortier et al. 2001). Furthermore, the attenuation of light means that, even during continuous illumination, the deeper layers provide safer environments to the threat of visual predation (Fiksen and Carlotti 1998). In effect, the ultimate causes for zooplankton migration would still exist since individuals that move between upper and deeper layers on a regular basis would be likely to have increased fitness. What becomes apparent is that a distinction must be made between synchronized vertical migrations of populations and the vertical migration of individuals. Although there is good evidence to believe that the former does not occur during summer in the arctic, there is no reason to exclude the possibility that individuals within populations are vertically migrating in an unsynchronized manner. Indeed, such “foray” type behavior has been hypothesized even in environments that do not experience continuous light levels, such as temperate Pacific and North Atlantic (Pearre 1979; Tarling et al. 2002).

Detecting foray behavior in zooplankton is difficult because it is impossible to track individuals over any length of time in situ (Pearre 2003). Many arctic studies have deployed depth discrete nets or have used echosounders (Dale and Kaartvedt 2000; Fortier et al. 2001), but these are only capable of monitoring the movements of populations over time. Some studies in temperate regions have examined the gut contents of individuals caught in the deeper layers to determine whether they contain surface-living prey items (Pearre 1973), but this demands specialized taxonomic knowledge and a level of net sampling resolution difficult to achieve in extreme environments such as the arctic. The acoustic Doppler current profiler (ADCP) is becoming increasingly used to obtain behavioral information on zooplankton that can help interpret the movements of individuals in populations (Tarling et al. 2001). The ADCP has the capacity to measure the velocity of zooplankton in the vertical plane through measuring Doppler shift (Plueddemann and Pinkel 1989). The product is a measurement of the average swimming behavior of individuals rather than the bulk movements of populations (Tarling et al. 2002). Logistically, ADCPs are an ideal instrument for deployment in extreme environments since

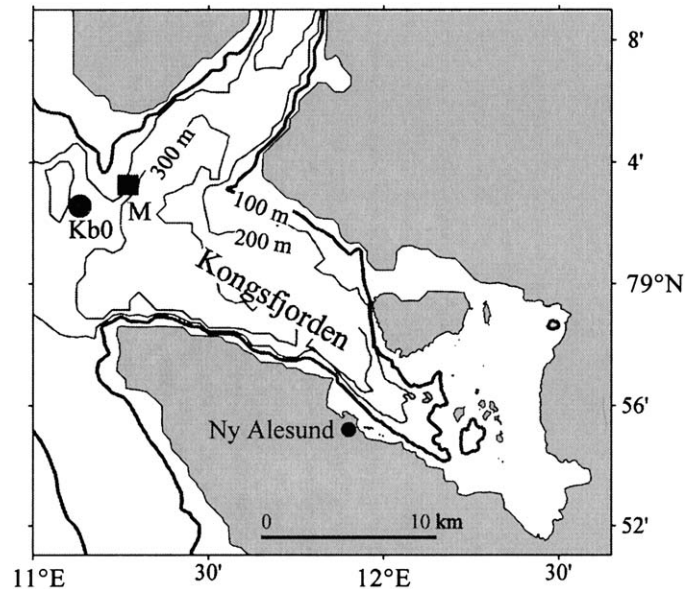


Fig. 1. Location map of Kongsfjorden showing the position of the mooring (M) and the zooplankton sampling station (Sta. Kb0). Irradiance measurements were made at Ny Alesund.

they can operate autonomously for periods in excess of 6 months, making continuous measurements at high temporal (<5 min) and spatial (4 m of water column) resolutions.

Our study site in Kongsfjorden in northwest Spitsbergen (Fig. 1) provided many advantages for the study of zooplankton vertical migration under arctic conditions. First, the sun does not set at this high-latitude location (79°N) for 4 months, with relatively high illumination for much of that time. Second, Kongsfjorden has high biomass of zooplankton that exhibit vertical migration, such as the copepods *Calanus finmarchicus* and *C. glacialis* and the euphausiid *Thysanoessa* spp. or the hyperiid amphipods *Themisto abyssorum* and *T. libellula* (Hop et al. 2002; Kwasniewski et al. 2003; Willis et al. in press). Third, the proximity of, and exchange with, Atlantic water in the West Spitsbergen Current maintains an open-water environment allowing mooring deployments and accompanying net catches to be undertaken during summer and autumn.

In this study, we examined the vertical migration behavior in Kongsfjorden between July and September, a period when zooplankton is abundant and activity levels are high. This period was also suitable for its physical attributes. At the start of the observational period, the sun remained at a high angle at midnight, and the light levels, although varying on a diel cycle, remained at relatively high values throughout, with no rapid rate of change in illumination. By the end, the sun began to set, providing a period of true darkness. The behavioral responses of zooplankton to continuous light and then to a light:dark cycle could be compared. Hydrographically, this period is characterized as being stable with the annual exchange of Atlantic and fjordic waters occurring earlier in the year (Cottier et al. 2005). This means that the possibility of

observed temporal changes in behavior being the result of immigration or emigration of populations can be excluded.

Our choice of study site and sampling period has given us a unique insight into some of the fundamental mechanisms that influence zooplankton vertical migration behavior. In particular, we are able to examine migratory behavior over a period in which there is a major shift in the light regime, from continuous illumination to nighttime darkness. Furthermore, our use of Doppler technology allows us to examine the vertical movement of individuals as well as of populations. Ultimately, we reexamine the question of whether vertical migration behavior in individual zooplankton continues to take place in arctic environments during periods of continuous light.

## Methods

**Sampling location**—Kongsfjorden is a glacial fjord on the northwest coast of Spitsbergen in the Svalbard archipelago. It is a multibasin fjord that is open to the West Spitsbergen Shelf through a common mouth it shares with the adjacent Krossfjorden (Fig. 1). The sampling area for this study was in the common mouth of the Kongsfjorden–Krossfjorden system. Here we give a brief summary only of the pertinent physical characteristics of the fjord (for a more extensive review, see Svendsen et al. 2002). The West Spitsbergen Shelf is a region where Atlantic, arctic, and glacial waters converge, mix, and are exchanged, and consequently, Kongsfjorden displays many subarctic characteristics despite its high-latitude location at 79°N. The hydrographic balance shifts seasonally such that, within an annual cycle, the shelf waters and adjacent fjords can switch from a state of arctic dominance (cold and fresh) to one of Atlantic dominance (warm and saline) and back (Cottier et al. 2005). Kongsfjordrenna, a submarine glacial trough, acts as the deep-water connection between the outer basin of Kongsfjorden and the shelf, so water mass exchange across the shelf–fjord boundary is not impeded topographically.

The zooplankton community of Kongsfjorden reflects the concurrence of Atlantic and arctic water masses such that species abundance and community structure is determined largely by exchange and advection (Kwasniewski et al. 2003; Willis et al. in press). Species representative of Atlantic water masses include the copepods *Calanus finmarchicus* and *Oithona atlantica*, the hyperiid amphipod *Themisto abyssorum*, and *Thysanoessa* spp. Species of arctic origin include the copepods *C. glacialis*, *C. hyperboreus*, and *Metridia longa*, the hyperiid amphipod *Themisto libellula*, the pteropod *Clione limacina*, and bivalve veliger *Limacina helicina*. Among these, the three *Calanus* species, *C. hyperboreus*, *C. glacialis*, and *C. finmarchicus*, are, by virtue of their high abundance and high lipid content, of major importance in the arctic food web (Scott et al. 2000; Falk-Petersen et al. 2001). *C. finmarchicus* and arctic *C. glacialis* in Kongsfjorden consist of local and advected individuals, with the proportions of each varying seasonally and annually depending on the timing and volume of Atlantic and arctic water intrusions. *Thysanoessa* spp. are also important components of the high-arctic food webs,

particularly of regions with increased levels of primary production (Falk-Petersen et al. 1981; Dalpadado and Skjoldal 1991). Hyperiid amphipods are generally ranked third in numerical abundance behind copepods and euphausiids (Bowman et al. 1982), although they may become a dominant component of fjordic environments at various times (Dalpadado 2002; Willis et al. in press).

**Mooring**—Two deployments of a single point multiparameter mooring were made at position 79°3.25'N, 11°18.0'E between April and September 2002 in 215 m depth of water (indicated by a square in Fig. 1). For full details of the mooring deployments and instrumentation, refer to Cottier et al. (2005). This work is based on the second deployment, which was made from the RRS *James Clark Ross* on 03 July 2002 and recovered on 28 September 2002 by RV *Håkon Mosby*. Temperature and salinity data from the mooring and from CTD profiles have been used to interpret the hydrographic changes during the deployment period (Cottier et al. 2005).

An upward-looking 300 kHz RDI broadband WH-ADCP was positioned on the mooring at a depth of 152 m. It was set to record data continuously in 30 depth “bins,” each 4 m depth, averaged over 33 pings every 4 min (giving a standard deviation in velocity measurements of 5 mm s<sup>-1</sup>). The depth range of the ADCP bins was 148–28 m; therefore, the instrument did not ensonify the entire water column, nor did it sample the surface layer. A data quality check based on signal:noise was applied by using the RDI correlation index recorded at the instrument.

The mean vertical velocity measured by the ADCP during the mooring deployment showed a small bias toward downward velocities. This was subtracted from the data to give the Doppler vertical velocity anomaly, which is recognized as a better representation of the temporal changes in the actual vertical migration speeds of the scatterers (Plueddemann and Pinkel 1989; Tarling et al. 2002). Echo intensity data collected by the ADCP were converted to absolute volume backscatter (Sv) measured in decibels by using the method described by Deines (1999) and adopted by Tarling et al. (2002). The ADCP operated successfully for 78 d representing 11 weeks of data. Vertical velocity anomaly and absolute backscatter time series were low-pass filtered, and a sequence of 11 profiles representing a mean 24-h period was calculated by averaging data from consecutive 7-d ensembles. These 11 profiles are the mean 24-h profiles for weeks 1 to 11 of the deployment.

**Irradiance**—Global solar irradiance measurements (W m<sup>-2</sup>) were available from the permanent weather station in Ny Ålesund for the duration of the mooring deployment. Data were recorded every minute and were extracted from the database of meteorological observations maintained by the Alfred Wegener Institute. Data return was >97% and postprocessed by applying a low-pass filter. The instrument was capable of resolving irradiance changes <0.1 W m<sup>-2</sup>, but the resolution of the archived data was 0.1 W m<sup>-2</sup>. Eleven mean 24-h irradiance curves for the weeks corresponding to the mean ADCP profiles were calculated by averaging data over seven consecutive days.

Table 1. Depth discrete concentration (individuals  $m^{-3}$ ) and predicted backscatter (Sv) of late developmental stages of three *Calanus* species found in Kongsfjorden. Net hauls were taken on 29 July and 21 September 2002 at Sta. Kb0 (Fig. 1).

	Depth (m) in July					Depth (m) in September				
	0–20	20–80	80–160	160–220	220–320	0–25	25–80	80–175	175–250	250–310
<i>C. finmarchicus</i>										
AM					1.9					
AF	6.6	0.1	3.4	1.5	24.3	2.3	0.6	0.3	0.8	9.2
CV	39.8	8.4	44.0	23.4	187.3	20.2	22.2	15.0	116.0	229.3
CIV	46.4	31.6	54.1	6.6		47.2	22.4	1.5	11.9	11.8
CIII	26.5	44.3	13.5		1.9	70.5	19.5	1.3		
CII	33.2	19.0	3.4			101.6	12.3	0.1	1.7	
CI	185.7	25.3				70.1	5.2			2.6
<i>C. glacialis</i>										
AM										
AF	0.4		0.3	1.5	1.9		0.6		0.1	5.3
CV	46.4	6.3	23.7	11.7	28.1	2.4	0.1	4.6	43.4	44.5
CIV	46.4	23.2	15.2	2.2	1.9				1.9	
CIII		4.2		0.7						
CII		2.1								
CI	73.0	12.7				4.6	2.3			
<i>C. hyperboreus</i>										
AF			0.1	0.1	1.1				0.1	0.5
CV				0.4	3.1		0.1		0.2	2.2
CIV	2.0	4.2		5.9	41.2	0.6	0.1	0.1	13.1	43.2
CIII				0.7		0.3			1.7	
Total concentration (ind. $m^{-3}$ ) CIII to A of all 3 species of <i>Calanus</i>	214.5	122.3	154.3	54.7	292.7	143.5	65.6	22.8	189.2	346
Predicted Sv of <i>Calanus</i> CIII to A, based on applying a TS of $-104.87$ dB to Eq. 1	$-81.6$	$-84.0$	$-83.0$	$-87.5$	$-80.2$	$-83.3$	$-86.7$	$-91.3$	$-82.1$	$-79.5$

**Zooplankton**—There was no systematic day/night net catch sampling contiguous with the ADCP data. However, single-net hauls close to the mooring in July and September 2002 resolved the afternoon depth distribution of the three major *Calanus* species. Sampling was conducted on 29 July 2002 at 14:30 h UTC and 21 September 2002 at 15:20 h UTC from RV *Oceania* and RV *Jan Mayen*, respectively. The sampling location was Sta. Kb0 ( $79^{\circ}03.00'N$   $11^{\circ}8.00'E$ ), 3.5 km to the southwest of the mooring (Fig. 1). Zooplankton were sampled at five distinct depth levels with a multiplankton sampler (mesh size =  $180 \mu m$ , opening  $0.25 m^2$ ). All samples were preserved in 4% formalin in seawater buffered with hexamine. Sorting and identification were carried out according to the procedure described by Falk-Petersen et al. (1999). The various species of *Calanus* were identified and then staged according to morphology and prosome lengths detailed by Kwasniewski et al. (2003).

“Forward-problem” estimates of zooplankton backscattering strength—The backscattering strength (Sv, dB) of zooplankton was predicted from combining the net-catch estimates of concentration (C, ind.  $m^{-3}$ ) with estimated target strength (TS, dB) as follows:

$$Sv = 10 \log(C) + TS \quad (1)$$

TS was estimated for *Calanus* at 300 kHz by using the randomly oriented fluid bent-cylinder model (Stanton et al. 1994):

$$TS = 10^{0.08R^2L^2\beta_D^{-1} [1 - \exp(-8\pi^2f^2D^2s^2c^{-2}) \cos(\pi f D c^{-1} (4 - \frac{1}{2}\pi(\pi f D c^{-1} + 0.4)^{-1}))]} \quad (2)$$

where  $R$  = reflection coefficient = 0.058 (Greene et al. 1998),  $L$  = body length (m),  $s$  = standard deviation (SD) of length  $\cdot$  length $^{-1}$ ,  $\beta_D$  = ratio of body length to width,  $D$  = body width (m),  $f$  = acoustic frequency in Hz =  $300 \times 10^3$ , and  $c$  = speed of sound =  $1500 m s^{-1}$ .

An average  $L$  for *Calanus* was calculated assuming that the population was made up of 3% adults, 60% CV, 27% CIV, and 11% CIII, following Table 1. Prosome lengths ( $L$ ) were, respectively, 3.05 mm, 2.66 mm, 2.10 mm, and 1.65 mm (using Marshall and Orr 1955). This gave an average  $L$  of 2.41 mm and SD of 0.37 mm. The ratio of length to width ( $\beta_D$ ) was 2.72 (Marshall and Orr 1955), making the average width ( $D$ ) 0.88 mm. Accordingly, the TS for *Calanus* at 300 kHz was  $-104.88$  dB. [2]

## Results

Hydrographic conditions at the mooring site during 2002 are described and discussed fully by Cottier et al. (2005).

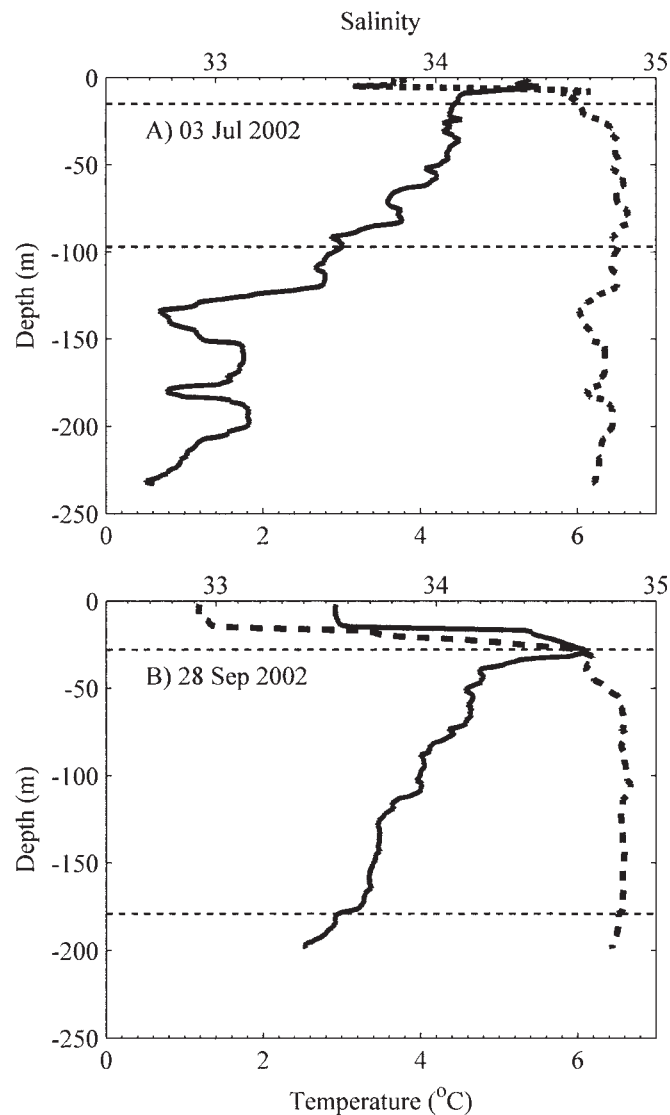


Fig. 2. Profiles of temperature (solid line) and salinity (dotted line) from the mooring location for (A) 03 July 2002 and (B) 28 September 2002. The Atlantic water layer is demarcated by the horizontal dashed line.

There were no significant shifts in water mass composition at the site over the course of the study, although some gradual changes were observed. In July, at the start of the mooring deployment, Atlantic water was present in the fjord mouth below the fresher surface-water layer and down to 100 m (Fig. 2A). The layer of Atlantic water remained as the dominant water mass and deepened from 100 m to 180 m over the duration of the study (Fig. 2B). Above this, the surface-water layer deepened to about 30 m, though there were occasions when this layer was observed to be deeper through halocline adjustment in response to fjord winds.

Figure 3 shows the mean 24-h curves of global irradiance and illustrates the seasonal changes occurring throughout the deployment period. Peak irradiance decreased from approximately  $400 \text{ W m}^{-2}$  during week 1 to less than

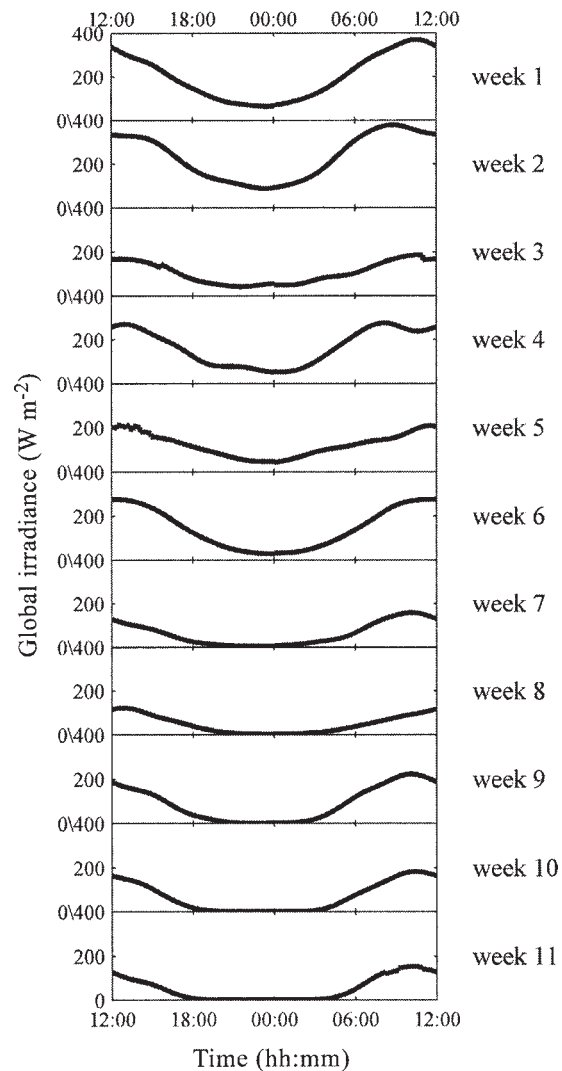


Fig. 3. The stacked plots are the mean 24-h global irradiance curves for weeks 1–11 derived from pyranometer data collected in Ny Ålesund. Time is UTC. Note that local noon is 48 min in advance of 12:00 h UTC.

$200 \text{ W m}^{-2}$  by weeks 10 and 11. Minimum irradiance during a mean 24-h period decreased from approximately  $70 \text{ W m}^{-2}$  in week 1 to the first occurrence, in week 8, of irradiance less than the resolution of the pyranometer data ( $0.1 \text{ W m}^{-2}$ ). The first occurrence of darkness in the raw data occurred in week 7 with mean irradiance approaching zero.

Net catches were successful in capturing three species of *Calanus* (Table 1) but some larger taxa, such as euphausiids and hyperiid amphipods, were absent. Of the three *Calanus* species, *C. finmarchicus* and *C. glacialis* were numerically dominant. *C. finmarchicus* was most abundant within each depth level in both months and constituted 60% and 80% of the total *Calanus* abundance in July and September, respectively. *C. glacialis* was the next most abundant, at 35% in July and 10% in September. Figure 4 shows a clear bimodal depth distribution for *C. finmarchicus* in both July and September but not for *C. glacialis*, which showed

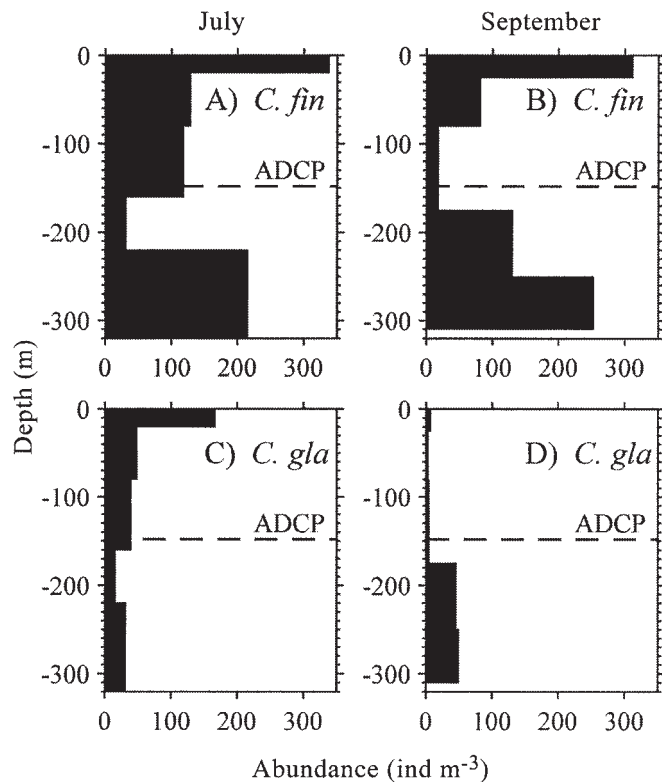


Fig. 4. Daytime vertical distribution in the abundance (ind.  $m^{-3}$ ) of (A, B) *Calanus finmarchicus* (*C. fin*) and (C, D) *C. glacialis* (*C. gla*) at Sta. Kb0 in the entrance to Kongsfjorden in July and September 2002. The level of the ADCP is marked by the horizontal dashed line.

greater surface abundance in July and greater abundance in deep water in September.

When all three *Calanus* species (stages CIII to adult) were combined, concentrations ranged between 22.8 ind.  $m^{-3}$  and 346.0 ind.  $m^{-3}$ , with the highest concentrations in the uppermost and lowermost parts of the water column (Table 1). Typical concentrations found in the midwater column were 122 ind.  $m^{-3}$  in July (20–160 m) and 65.6 ind.  $m^{-3}$  in September (20–175 m). By using a TS of  $-104.88$  dB (see above), the equivalent backscattering strength (Sv) of these concentrations were predicted to be between  $-87.5$  dB and  $-79.5$  dB (Table 1). In the midwater column, Sv was predicted to be  $-84.0$  dB in July (20–80 m) and  $-86.7$  dB in September (25–80 m).

Mean 24-h profiles of absolute backscatter (Sv) for consecutive weeks of the mooring deployment are presented in Fig. 5. The  $-86$  dB contour was used to delineate regions of enhanced backscatter and sound-scattering layer (SSL) boundaries. Patterns in the backscatter profiles can be divided into two distinct periods. During weeks 1–6, backscatter greater than  $-86$  dB occurred consistently in the upper part of the water column at about 50 m but becoming slightly deeper by week 6. In contrast, during weeks 7–11, backscatter greater than  $-86$  dB was detected in the deeper water of the mooring location. During this later period, the depth variation of the  $-86$  dB contour was

consistent with a diel vertical migration (DVM) pattern as the SSL moved into shallower water after noon, followed by a descent into deeper water. Through this second period, the ascending and descending SSLs became more distinctive. When weeks 8 and 11 are contrasted (Fig. 5), the ascent and descent periods become well defined by the  $-86$  dB contour. The concentration of migrating animals into these periods during week 11 reduces the backscatter in the water below 50 m to background levels between 18:00 and 02:00 h.

Mean 24-h profiles of Doppler vertical velocity anomaly ( $w'$ ) for each week of the mooring deployment are shown in Fig. 6. Through weeks 1–5, there is almost total data coverage through the effective range of the ADCP. From week 6 onward, there is increasing data dropout from the upper bins (white segments in the profiles) as the signal:noise ratio falls below the allowed threshold. The most likely cause for this is a relatively low concentration of small scatterers near the surface producing a weak return echo. During daytime hours, dropout is particularly prevalent as scatterers concentrating close to the instrument absorb a lot of energy in the pulse emitted by the ADCP.

A general feature of the mean 24-h profiles of  $w'$  is that they have a two-layer structure with predominantly downward velocities (dark gray shades) in the upper part and upward velocities (light gray shades) in the lower part. This feature is particularly evident in weeks 1–3 and 6–9. The depth of the interface between these two layers changes according to the time of day, being at about 80–100 m during daytime and moving up to 40–60 m during nighttime. The mean upward and downward  $w'$  in each layer were of similar magnitude each week at around  $\pm 1$   $mm\ s^{-1}$ . The exception was week 7 with mean  $w'$  values of  $+1.7$   $mm\ s^{-1}$  and  $-2.9$   $mm\ s^{-1}$ . Peak upward velocities were generally about  $+3$  to  $+4$   $mm\ s^{-1}$ , with the greatest upward velocities occurring in weeks 10 and 11 at  $+8.5$   $mm\ s^{-1}$  and  $+6.0$   $mm\ s^{-1}$ , respectively. Instances of enhanced upward (greater than  $+3$   $mm\ s^{-1}$ ) or downward (less than  $-3$   $mm\ s^{-1}$ ) velocities are demarcated by regions of lighter and darker shading, respectively. For each week, the peak downward velocities were generally greater in magnitude than peak upward velocities.

In Fig. 6, upward vertical velocity contours only are drawn at  $+2$ ,  $+4$ , and  $+6$   $mm\ s^{-1}$ . The minimum vertical velocity contour of  $+2$   $mm\ s^{-1}$  is greater than the mean upward  $w'$  for each week and is approximately equal to the theoretical precision of  $w'$  averaged over a week ( $5/\sqrt{7}$   $mm\ s^{-1}$ ). Therefore, it is indicative of enhanced upward vertical migration. Before week 7, there were few and sporadic occasions when  $w'$  exceeded  $+2$   $mm\ s^{-1}$ . By week 7, the  $+2$   $mm\ s^{-1}$  contour shows that there were multiple occasions throughout the day when upward  $w'$  was greater than the mean. During weeks 8–11, the occurrence of increased upward  $w'$  became more closely confined in time to the period between 18:00 h and midnight. In weeks 10 and 11, the period of increased upward  $w'$  was followed by a period of predominantly downward velocities. During weeks 8 and 9, the two-layer structure and the period of

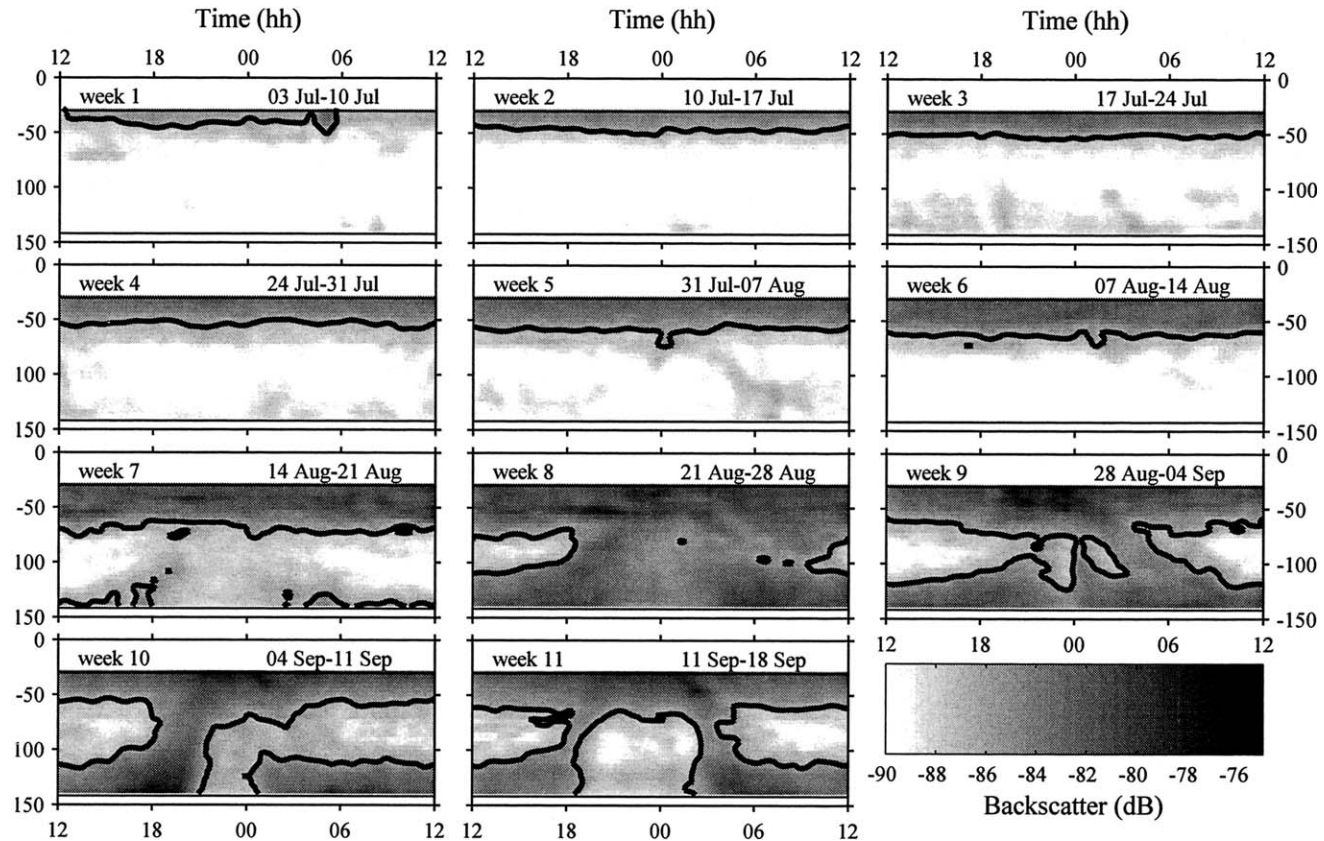


Fig. 5. Mean 24-h profiles of absolute backscatter (dB) for consecutive weeks from 03 July to 18 September 2002 plotted against depth and hour of the day (UTC). Each profile is labeled with a week number (1–11) and the corresponding dates. The backscatter contour of  $-86$  dB marking the edge of the SSL is drawn in black.

increased  $w'$  both occur, indicating a period of transition between two behavioral patterns.

Averaging the Doppler vertical velocity anomaly ( $w'$ ) over the range of the ADCP at each time step yields a depth-averaged vertical velocity anomaly for each week of data. The theoretical precision of this value (assuming at least 20 bins are available) is approximately  $0.4 \text{ mm s}^{-1}$  ( $5/(\sqrt{7} \cdot \sqrt{20}) \text{ mm s}^{-1}$ ). During weeks 1–6, depth-averaged  $w'$  oscillated consistently around zero, the mean being  $0.0 \pm 0.4 \text{ mm s}^{-1}$ ; an example of this is week 6, which is plotted in Fig. 7. For weeks 7–11, there were extended periods when depth-averaged  $w'$  was significantly greater or less than zero at the 99% confidence level; data from these periods are also plotted in Fig. 7.

Periods of significant positive depth-averaged  $w'$  started in week 7 and continued into week 11. It is perhaps significant that it was during week 7 when irradiance was sufficiently low that levels approached the detection limit of the pyranometer for the first time during the mooring deployment. Extended periods of significant negative depth-averaged  $w'$  occurred in weeks 10 and 11 only. In general, the periods of positive depth-averaged  $w'$  occurred before midnight, while periods of negative depth-averaged  $w'$  occurred after midnight. Both positive and negative periods were asymmetric, with the peak in positive values occurring during the second half of the period and the peak

in negative values occurring in the first third of the period. The duration for which depth-averaged  $w'$  was significantly greater than zero decreased from 6 h in week 8 to 4 h by week 11. Peak positive depth-averaged  $w'$  occurred progressively earlier in the day, from 00:00 h in week 7 to 19:15 h in week 11. Further, peak values in depth-averaged  $w'$  increased from  $1.5 \text{ mm s}^{-1}$  in week 8 to  $5.3 \text{ mm s}^{-1}$  in week 10. Negative depth-averaged  $w'$  occurred over a longer duration than positive depth-averaged  $w'$  for the same week and comprised a time of peak descent followed by a number of secondary descents.

A synthesis of the surface irradiance data and depth-averaged  $w'$  for weeks 7 to 11 is presented in Fig. 8. Onset and duration of darkness (times when irradiance fell below detection limits) and the relative rates of change in irradiance ( $\Delta E/E$  [%  $\text{min}^{-1}$ ]) were calculated by using the mean 24-h curves in Fig. 3. The maximum value of  $\Delta E/E$  was often smaller than the detection accuracy of the instrument or very poorly defined in time as a result of the rather gradual changes in irradiance at this latitude (Fig. 9). The first well-defined maximum value for  $\Delta E/E$  was obtained in week 8. Further, the surface irradiance at the start of positive depth-averaged  $w'$  was determined for weeks 8–11. Sunset first occurred during week 8, and mean time of sunset for Ny Ålesund for successive weeks was derived from the U.S. Naval Observatory (<http://aa.usno.navy.mil/>). These irradiance parameters for weeks 8–11 are

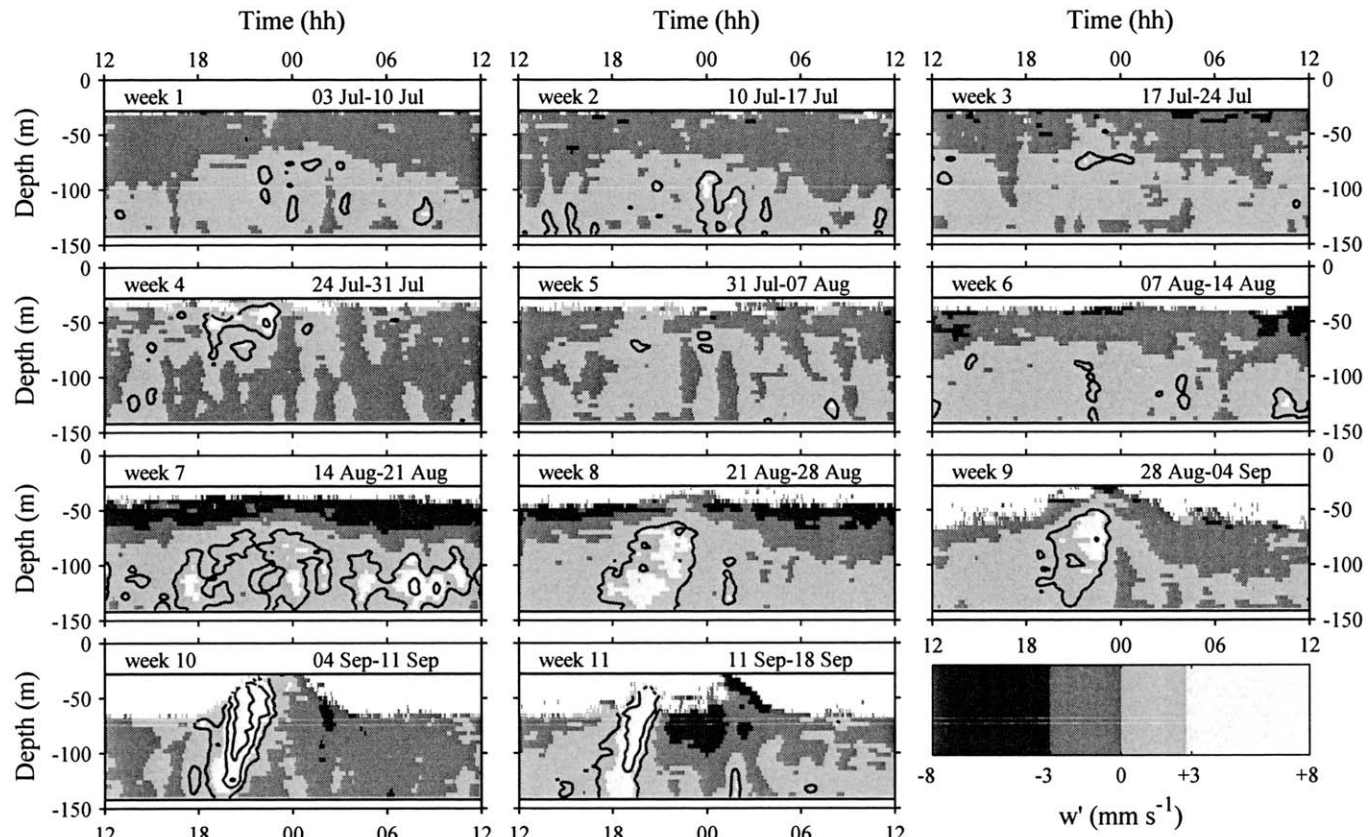


Fig. 6. Mean 24-h profiles of Doppler vertical velocity anomaly ( $\text{mm s}^{-1}$ ) for consecutive weeks from 03 July to 18 September 2002 plotted against depth and hour of the day. Each profile is labeled with a week number (1–11) and the corresponding dates. Upward velocities (positive) are denoted by light gray shades, and downward velocities (negative) are denoted by dark gray shades. Contour lines are drawn in black for upward velocities only at +2, +4, and +6  $\text{mm s}^{-1}$ .

summarized in Table 2. Week 7 is not included in the table because although irradiance levels fell below detection limits on one occasion during that week, other irradiance parameters based on the mean 24-h data are not defined.

Figure 8 shows the clear progression in duration of darkness and time of sunset. In weeks 9–11, the time of sunset precedes the time of maximum  $\Delta E/E$  by up to 20 min, which is itself closely coincident with the onset of darkness. Positive depth-averaged  $w'$  ends well before the cessation of the dark period. The simple correspondences between parameters does not hold true for week 8, suggesting that  $\Delta E/E$  and the onset of darkness are poorly defined for the mean irradiance curve in this week. The start of positive depth-averaged  $w'$  occurs when irradiance is less than  $50 \text{ W m}^{-2}$  for weeks 8–11 and the time of peak depth-averaged  $w'$  occurs between 25 and 50 min after the time of maximum  $\Delta E/E$  as measured at the surface (Table 2).

Figure 9 combines two ADCP parameters, absolute backscatter ( $S_v$ ) and vertical velocity anomaly ( $w'$ ), for weeks 8–11. The  $+3 \text{ mm s}^{-1}$   $w'$  contour is overlaid onto the mean 24-h  $S_v$  profiles for each week. The  $+3 \text{ mm s}^{-1}$  contour is a useful indicator of vertical migration during these weeks because it is greater than the mean upward  $w'$  for each week but less than the peak value of  $w'$ . For each

of the 4 weeks,  $w'$  exceeds  $+3 \text{ mm s}^{-1}$  at some time during the interval 18:00 to 00:00 h. Except for week 9, the  $+3 \text{ mm s}^{-1}$  contour originates from the deep water and rises quickly through the water column with time. The critical observation here is that in all cases, the time of enhanced upward vertical velocity at a given depth level lags behind the leading edge of the SSL. This is seen most clearly in weeks 10 and 11, when the peak  $w'$  occurs toward the trailing edge of the SSL.

This lagging effect between backscatter and vertical velocity is illustrated more clearly in Fig. 10 by using data from week 10 with contours of positive  $w'$  overlaid by the  $-86 \text{ dB}$  contour. The highest values of  $w'$  are found toward the trailing edge of the SSL, as is the time of peak depth-averaged  $w'$  (indicated by the triangle). Two oblique lines (A and B) overlay the  $-86 \text{ dB}$  contour, and their gradients can be used as an estimate of the vertical ascent rate of the SSL (Tarling et al. 2001). Line A corresponds to the SSL rising through the water column at  $1.2 \text{ mm s}^{-1}$ , and line B corresponds to  $6.7 \text{ mm s}^{-1}$ . The passage of the migrating scatterers takes about 4 h to pass through the 85-m depth level. If these speeds are roughly constant over time and depth, it requires some of the migrators to have started their ascent 100 m below the uppermost ADCP bin, implying that they were residing below the ADCP depth during the day.

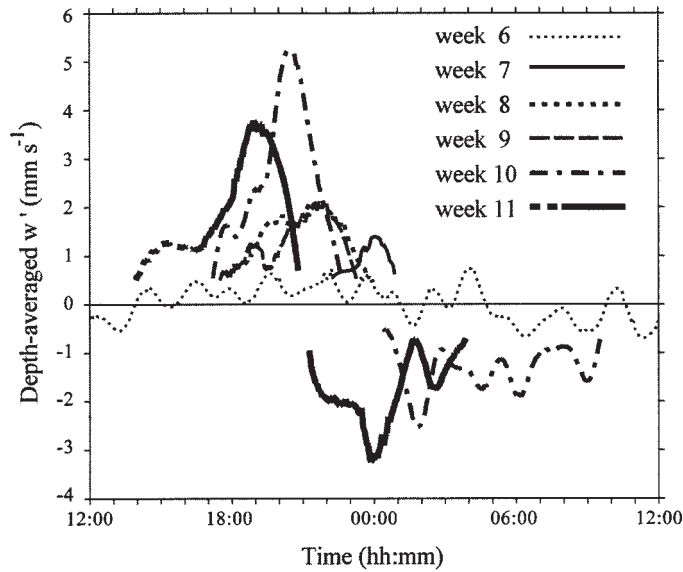


Fig. 7. Depth-averaged Doppler vertical velocity anomaly plotted for weeks 6–11. Week 6 is illustrative of weeks 1–6 of the study period where the depth-averaged vertical velocity oscillated around  $0 \text{ mm s}^{-1}$ . Although the data for weeks 7–11 are continuous, only those periods when the depth-averaged vertical velocity was significantly greater or less than zero at the 99% level are plotted. The dashed portion of the data line from week 11 is used to indicate a time of rather limited ascent before the main migration period.

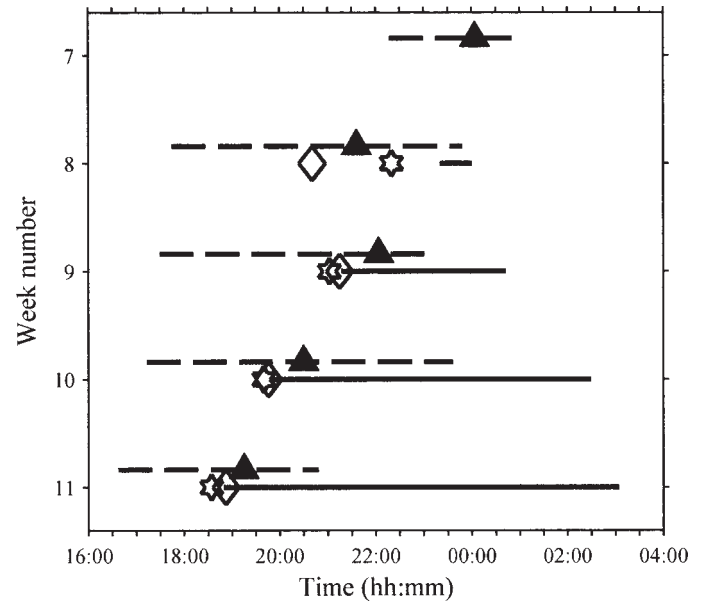


Fig. 8. Synthesis of the depth-averaged Doppler vertical velocity anomaly from Fig. 7 and irradiance for weeks 7 to 11. Dashed lines indicate period of significant positive depth-averaged Doppler vertical velocity anomaly with the triangle marking the time of peak velocity. The black lines denote the duration of darkness when  $E < 0.1 \text{ W m}^{-2}$ , with the times of sunset (star) and maximum  $\Delta E/E$  (diamond) indicated. Numeric values for these parameters are given in Table 2.

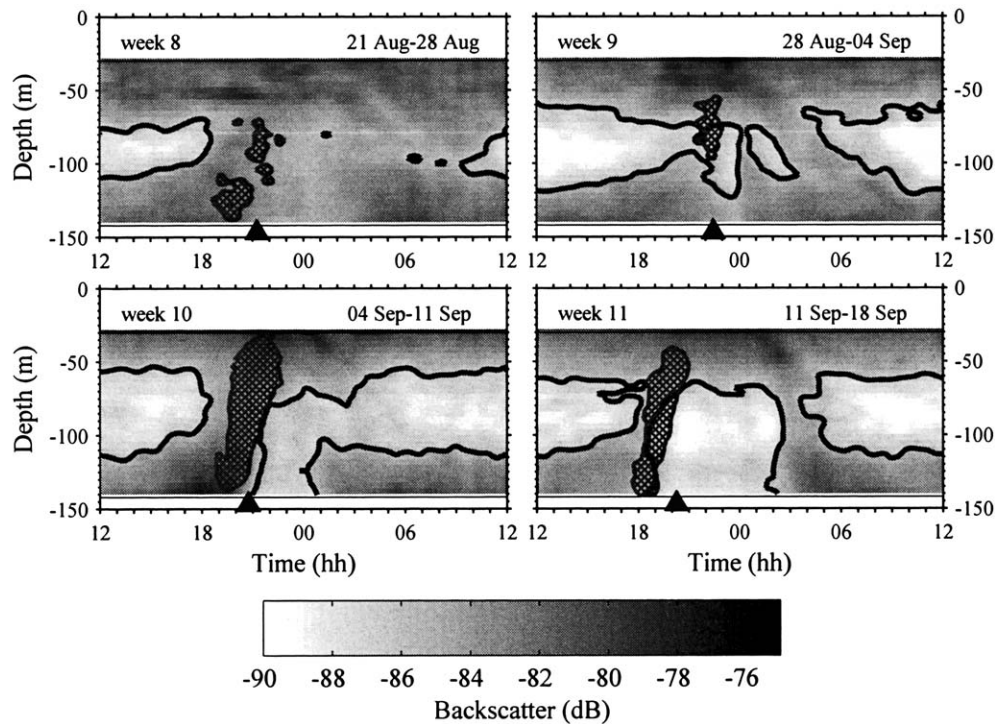


Fig. 9. Mean 24-h profiles of absolute backscatter (dB) for weeks 8 to 11 plotted against depth and hour of day. The backscatter contour of  $-86 \text{ dB}$  marking the edge of the SSL is drawn as a heavy black line. The dark-hatched areas in each plot mark the periods where the Doppler vertical velocity anomaly was greater than  $+3 \text{ mm s}^{-1}$ , which indicates of enhanced vertical migration. The triangles along the x-axis indicate the times of peak upward depth-averaged vertical velocity as determined from Fig. 7.

Table 2. Irradiance parameters for weeks 8 to 11 based on global irradiance data from Ny Ålesund and sunset tables. Sunset times are given for the middle day of the week and irradiance is measured in  $\text{W m}^{-2}$ . All times are UTC.

Parameter	Week			
	8	9	10	11
Sunset (midweek)	22:20 h	21:02 h	19:40 h	18:34 h
Onset of darkness ( $E \leq 0.1 \text{ W m}^{-2}$ )	23:20 h	21:27 h	19:48 h	18:49 h
Duration of darkness	40 m	3 h 25 m	6 h 40 m	8 h 15 m
Time of maximum $\Delta E/E$	20:41 h	21:15 h	19:46 h	18:52 h
Magnitude of max. $\Delta E/E$ ( $\% \text{ min}^{-1}$ )	1.1	2.3	2.0	2.5
Irradiance at start of positive depth-averaged $w'$	44	49	34	30

## Discussion

The ADCP data indicate that there was a change in the vertical migration behavior of zooplankton at a high latitude site between July and September. During this period the light environment changed from one of continuous sunlight to a true day–night contrast. In particular, we see evidence for unsynchronized migration of individual animals during the weeks of continuous daylight (weeks 1–6) changing to an increasingly synchronized migration of the population coinciding with the onset of darkness (weeks 7–11). The synchronized migration behavior recorded by the ADCP has a clear DVM pattern with ascent occurring at dusk followed by a descent phase.

We believe that much of the migrating zooplankton during weeks 1–6 are calanoid copepods, specifically

*Calanus finmarchicus* and *C. glacialis*. The most likely life stages to perform this vertical migration are CIV and CV. This statement is based on (1) their numerical dominance in Kongsfjorden, (2) their vertical distribution in the part of the water column encompassed by the ADCP, (3) the correspondence between the species life history and the ADCP pattern, and (4) the acoustic signature. Our “forward problem” prediction of the amount of backscatter ( $S_v$ ) resulting from *Calanus* in water column in July was relatively close to the  $S_v$  observed by the ADCP within both the uppermost depths (0–20 m;  $-81.6 \text{ dB}$  predicted;  $-80$  to  $-84 \text{ dB}$  observed) and the middepths (20–160 m;  $-84.0 \text{ dB}$  predicted;  $-88 \text{ dB}$  to  $-82 \text{ dB}$  observed).

Our observations that *C. finmarchicus* and *C. glacialis* numerically dominate the mesozooplankton community in Kongsfjorden agrees with those of Kwasniewski et al. (2003). They were also the most abundant calanoids in sediment trap material collected during the same mooring deployment (Willis et al. in press). Our net catches found that the older life stages had a bimodal distribution, being found in both the upper and lower parts of the water column. According to Kwasniewski et al (2003), individuals caught in the mid- and upper water column layers are probably the young stages of fjordic *C. finmarchicus*, that will continue to develop and grow over the course of the study period.

The backscatter profiles during weeks 1–6 in Fig. 5 show values remaining constant at all depths throughout the day indicating that there is no net diurnal change in the vertical distribution of scatterers. The same weeks 1–6 in Fig. 6 give a contrasting picture with diurnal variation in the profiles of vertical velocity anomaly ( $w'$ ); this variation is clearest in weeks 1–3 and 6. These profiles have a two-layer structure, with upward velocities persisting in the lower layer and downward velocities persisting in the upper layer throughout the 24-h period. The two layers are separated by an interface where the mean vertical velocity anomaly is zero. The depth of the interface varied diurnally, being deeper around midday and shallower around midnight, and the profiles show weekly variance in the depth range and occurrence of a clear two-layer structure. Candidate physical causes, such as tides or internal waves, can be disregarded as the data is averaged over a week, tending to smooth over these cyclic effects. We propose that migratory phenomena are the cause of these observations.

To interpret the two-layer distribution in  $w'$  and the significance of the diurnal variation in the depth of the zero

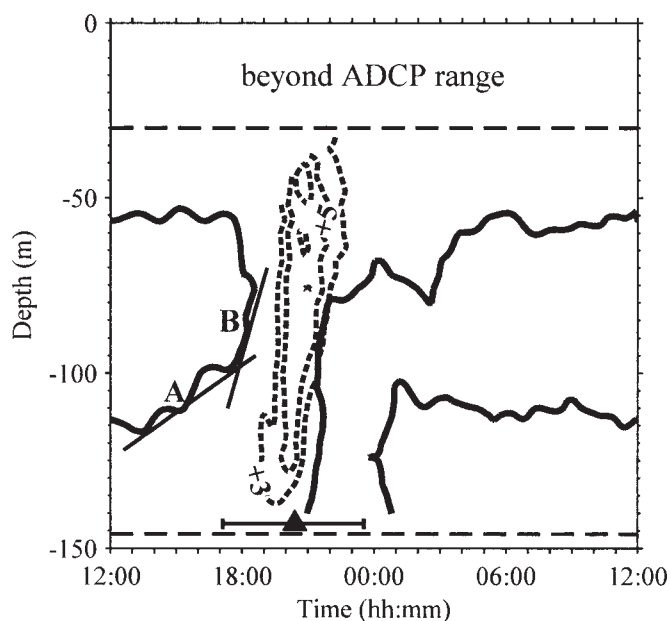


Fig. 10. Doppler vertical velocity anomaly data for week 10 (04 Sep–11 Sep) as a function of time and depth plotted as dotted contours at intervals of +3, +5, and +7  $\text{mm s}^{-1}$ . The overlaid solid line is the absolute backscatter contour of  $-86 \text{ dB}$ , indicative of the SSL. Oblique lines A and B represent the ascent gradient of the SSL. The horizontal bar close to the x-axis indicates the duration of positive depth-averaged vertical velocity anomaly, and the triangle marks the time of the peak value. Dashed horizontal lines denote the range of the ADCP.

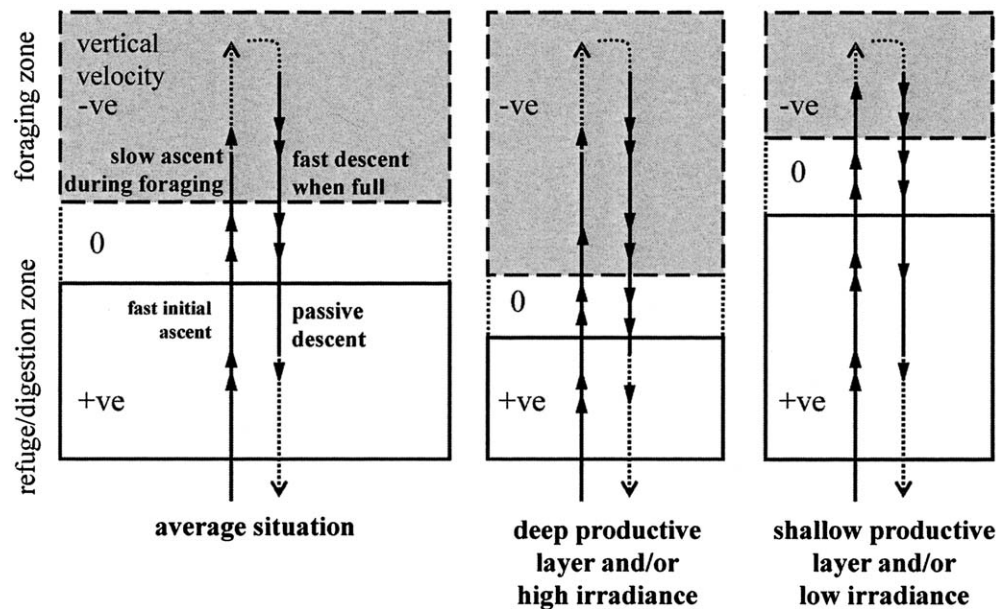


Fig. 11. Conceptual model of swimming behavior of copepods in a high arctic fjord. Negative net vertical velocities in the upper layers are a result of active downward swimming when full. Positive upward velocities in the deeper layers are a product of active upward swimming. Although the copepods are also migrating in the opposite direction in both layers, their velocities are slower (indicated by dotted lines) either because of foraging activity (upper layer) or passive descent (lower layer). The zero velocity layer is where the migration speed is equal in both directions. The vertical location of this zone will alter according to the depth of the productive layer and/or the level of irradiance.

interface, we must consider that the ADCP calculates the mean velocity of all scatterers in each bin (Plueddemann and Pinkel 1989). Consequently, scatterers may move simultaneously in opposite directions in the vertical plane but the vertical velocity measured at the ADCP will be a mean velocity; therefore, it does not necessarily correspond to a net migration of scatterers in the direction of the mean velocity vector. We can interpret these patterns with a conceptual model of migration based on commonly observed zooplankton behavioral strategies and illustrated schematically in Fig. 11. In the deeper layers, upward movement is often rapid (active) to reduce transit time through food-poor regions (Andersen and Nival 1991; Tarling et al. 2001), whereas downward movement is slow (passive) because predation risk is less (Fiksen and Carlotti 1998) and energy can be conserved (Minkina 1981). Assuming the flux of individuals in and out of this layer is equal, this would produce a net upward movement. Conversely, in the surface layers, upward movement is slow to reduce detection levels (Pearre 1970, 1973) and allow feeding (Atkinson et al. 1992), whereas downward movement is rapid to move away from risky layers when sated (Simard et al. 1985). This produces a net downward movement, assuming the net flux of individuals is constant. It is very likely that an individual will undertake multiple migrations in a day according to its own needs (Pearre 2003). Internal rates such as ingestion and digestion and swimming activity are therefore likely to play a major role in determining the frequency of vertical migrations in these situations.

The depth of the zero velocity interface (weeks 1–3 and 6) varies between midday and midnight in a manner similar to the irradiance curves of Fig. 3. We propose changes in zooplankton behavior in response to light levels are the cause of the diurnal variation. Conceptually, the interface will contain scatterers both ascending into a high risk zone and descending into a zone of lower risk. The interface marks the depth where ascending and descending individuals switch between fast and slow swimming in response to their trade-off strategy; it does not represent the upper limit of ascending animals. Weekly variations between  $w'$  profiles in weeks 1–6 are probably due to natural variations in phytoplankton, which determines food availability and light attenuation, and reduced irradiance through variability in cloud cover.

Our interpretation of Fig. 6 using a conceptual model of migration indicates that during times of continuous daylight *Calanus* species do perform vertical migration. This is an unsynchronized migration of individuals within a population rather than a synchronized migration of the entire population. It would appear that during continuous daylight, the animals are adopting a foray-type behavior with active swimming up and down to minimize the time spent in the high-risk, food-rich surface layers. This behavior was originally speculated on by Gauld (1953) and later adopted by Pearre (1973, 1979) and Mackas and Bohrer (1976) to explain their observations. Pearre (2003) referred to it as the “hunger/satiation” hypothesis and proposed that it may occur in a wide range of marine and freshwater taxa. The referred examples of Pearre (2003) all

contained a period of true nighttime, when animals were believed to make repeated migrations into the surface layers to feed and descend to digest and replenish digestive enzymes. Here we propose that foray behavior occurs even in full daylight. This raises the possibility that such behavior may also be exhibited during daytime in environments with conventional light:dark regimes.

Finding vertical migration behavior during periods of midnight sun is contrary to the conclusions of other studies of this situation. Both Dale and Kaartvedt (2000) and Fortier et al. (2001) used depth discrete net sampling as their main means of observing the behavior of the copepod population. Such nets are an effective means of determining species composition and size related patterns during synchronized vertical migrations when deployed at sufficiently frequent intervals (Wiebe et al. 1992). The data are unsuitable for detecting fluxes where there is no net change in the vertical distribution of the population (Pearre 2003). Fischer and Visbeck (1993) deployed a 153.6 kHz ADCP in the Greenland Sea and detected vertical velocity anomalies that changed seasonally. However, copepods cannot be detected by such a low sound frequency, and euphausiids were proposed as being the main contributor to the signals. Furthermore, their analysis did not achieve the same level of resolution as the present study, and the zero-velocity interface was not identified.

Beginning in week 7, we see the first evidence of synchronous migration. Figure 7 shows that the depth-averaged vertical velocity became significantly nonzero during week 7. Furthermore, SSLs with upward and downward trajectories, marked by the  $-86$  dB contour, become identifiable (Fig. 5). As these SSLs increase in coherence toward week 11, so their Sv correspondingly increases in value (more than  $-80$  dB). This increase in Sv may be the result of a number of factors: (1) an increase in the concentration of *Calanus*, (2) an increase in the average size of individuals, and (3) swarming responses in other, less abundant species such as the euphausiid *Thysanoessa* spp. or the hyperiid amphipid *Themisto* spp. The first scenario appears unlikely given that net catch concentrations of *Calanus* in September are lower than in July, particularly in the part of the water column where the Sv is highest (80–175 m). The second scenario is a better possibility because individuals will continue to grow over the summer months. However, we estimate that the average size of an individual would have to double in order to counteract the observed decrease in concentration. The third scenario is the most likely, particularly with respect to euphausiids, which are noted to form SSLs in other fjordic environments (Falk-Petersen and Kristiansen 1985; Simard et al. 1986; Tarling et al. 2002). Euphausiids are prolific swimmers (Kils 1981; De Robertis 2002), and their absence in the net catches taken in the vicinity of the ADCP mooring may be a result of their noted ability to avoid nets that are hauled too slowly, or may be a result of their small mouth diameters (Wiebe et al. 1982), as is probably the case in this instance.

Low abundances of *Thysanoessa* spp. have been reported in other parts of Kongsfjorden (Weslawski et al. 2000). Both *Themisto abyssorum* and *T. libellula* were observed in

sediment traps deployed in the fjord over the period of study (Willis et al. in press). Present understanding of the vertical distribution and vertical migration behavior of these organisms is limited. Falk-Petersen et al. (unpubl. data) did, however, record *T. libellula* performing DVM between 50 m and 150 m in Rijpfjorden in September 2004 on the northern island of Svalbard, Nordaustlandet. The increase in the abundance of *T. libellula* in sediment traps over the period when SSLs were starting to appear suggests that *T. libellula* may be contributing to the DVM pattern. The thecosomate pteropod *Limacina helicina* is a strong acoustic scatterer that increased in relative concentration over the study period. However, our net catches indicated that it resided mainly in the surface layers and was unlikely to be part of the migrating scattering layers.

As the weeks progress, it is apparent from Fig. 9 that enhanced upward vertical velocity anomaly and ascent of the SSL are linked phenomena. In all cases, the region of highest vertical velocity is associated with the trailing edge of the SSL, indicative of a coordinated population. To investigate the dynamics of the migrating population, we looked more closely at the trajectory of the SSL (Fig. 10) and the measured  $w'$ . The change in the incline of the  $-86$  dB contour from  $1.2$  to  $6.7$  mm s $^{-1}$  at about 17:30 h closely matches the start of the period of positive depth-averaged  $w'$  for week 10. To interpret the combined data sets, we must recall that the ADCP measures the mean velocity of all the scatterers in each bin (Plueddemann and Pinkel 1989), and nonmigrating scatterers will tend to bias estimates of vertical velocity to the low end. Although the leading edge of the SSL is ascending at  $6.7$  mm s $^{-1}$ ,  $w'$  at the leading edge is  $<3$  mm s $^{-1}$ . Here, there is probably a mix of fast- and slow-moving individuals, with the variation in speed being a product of the maintenance of spatial coherence—that is, individuals at the front are slowing down to avoid separation (Heywood 1996; Tarling et al. 2002). Toward the trailing edge of the SSL, vertical velocities are greater than  $6$  mm s $^{-1}$  and peak at  $8.5$  mm s $^{-1}$ , implying that all scatterers are ascending at or faster than the ascent rate of the population, with minimal downward bias. Here, almost all individuals swim at peak rates in order to not be left behind. The peak velocities at the trailing edge lie within the reported range of swimming speeds of *C. finmarchicus* ( $4.2$ – $18.3$  mm s $^{-1}$ ; Mauchline 1998, p. 410).

In Fig. 8, we have compared parameters of surface irradiance (summarized in Table 2) and depth-averaged vertical velocity anomaly (extracted from Fig. 7) to explore changes in light as a cue for synchronous behavior for weeks 7–11. Vertical migration commences when positive depth-averaged  $w'$  is significantly greater than zero, and this occurs well in advance of sunset. This is in contrast to observations by Fischer and Visbeck (1993) from the Greenland Sea; they observed upward motion beginning immediately after sunset. In our study, surface irradiance values at the start of upward migration are similar (ranging from  $30$  to  $50$  W m $^{-2}$ ), at approximately 10% of the midday irradiance values. When we take a mean value of  $40$  W m $^{-2}$ , we find that irradiance does not ever drop below this threshold during weeks 1 to 5 and is  $<40$  W m $^{-2}$  for

only 4 h in week 6 compared with nearly 12 h in week 7. Taking the lower limit of  $30 \text{ W m}^{-2}$ , irradiance drops below this level for only 40 min in week 6 compared with 10 h in week 7. Maximum depth-averaged  $w'$ , indicative of synchronous migration, occurs after sunset and after the point of maximum relative irradiance change. This result can be interpreted as the onset of vertical migration being cued by absolute light levels, as found by Roe (1983) and Frank and Widder (1997), whereas enhanced synchrony in the population is more closely linked to relative change in irradiance, as found by Ringelberg (1995). In such an interpretation, it is important to acknowledge that irradiance parameters observed at depth can vary significantly from those at the surface (Widder and Frank 2001). We consider our conclusions on the effects of light conditions on the triggering and synchrony of vertical migration to be appropriate in the absence of in situ measurements of irradiance through the water column.

A notable pattern that increasingly develops from weeks 7 to 11 is a concentrated period of downward velocities in the upper and middepth layers immediately after the arrival of the SSL. Tarling et al. (2002) noted a similar pattern in vertical velocity data collected by 300 kHz in the Clyde Sea. In that study, simultaneous net catches determined the main scatterer in the SSL to be the euphausiid *Meganycitiphanes norvegica*, while the only organism present in the region of high downward velocities around midnight was *Calanus finmarchicus*. Tarling et al. (2002) believed that *C. finmarchicus* swam downward to avoid the euphausiid, although it was unclear whether the threat of predation or the interference of the copepod's foraging behavior were the main driving forces. The lack of appropriate net catches prevents us from establishing the identity of the main scatterer in the SSL, although the similarity to the acoustic patterns observed in the Clyde Sea suggest that a similar scenario is taking place.

By using a Doppler technique in a unique high-latitude environment, we have been able to investigate the change in migratory behavior between conditions of midnight sun and true day–night contrast. During periods of continuous illumination, foray-type migration occurs, with individuals making many migrations toward the surface each day in an unsynchronized manner. The finding is a rare example of vertical migration continuing in the absence of clear proximal light-mediated cues. The pattern changes to a synchronized vertical migration of individuals once true nighttime resumes toward autumn. Most individuals synchronize their migrations with the maximum relative change in irradiance and maximize their fitness through foraging in the food-rich layers under the cover of darkness.

## References

- ANDERSEN, V., AND P. NIVAL. 1991. A model of the diel vertical migration of zooplankton based on euphausiids. *J. Mar. Res.* **49**: 153–175.
- ATKINSON, A., P. WARD, R. WILLIAMS, AND S. A. POULET. 1992. Feeding rates and diel vertical migration of copepods near South Georgia—comparison of shelf and oceanic sites. *Mar. Biol.* **114**: 49–56.
- BLACHOWIAK-SAMOLYK, K., S. KWASNIEWSKI, K. RICHARDSON, K. DMOCH, E. HANSEN, H. HOP, S. FALK-PETERSEN, AND L. T. MOURITSEN. 2006. Arctic zooplankton do not perform diel vertical migration (DVM) during periods of midnight sun. *Mar. Ecol. Prog. Ser.* **308**: 101–116.
- BOWMAN, T. E., A. C. COHEN, AND M. M. MCGUINNESS. 1982. Vertical distribution of *Themisto gaudichaudii* in a deepwater dumpsite 106 off the mouth of Delaware Bay. Smithsonian Institution Press.
- COTTIER, F. R., V. TVERBERG, M. E. INALL, H. SVENDSEN, F. NILSEN, AND C. GRIFFITHS. 2005. Water mass modification in an arctic fjord through cross-shelf exchange: The seasonal hydrography of Kongsfjord, Svalbard. *J. Geophys. Res. Oceans* **110**: C12005.
- DALE, T., AND S. KAARTVEDT. 2000. Diel patterns in stage-specific vertical migration of *Calanus finmarchicus* in habitats with midnight sun. *ICES J. Mar. Sci.* **57**: 1800–1818.
- DALPADADO, P. 2002. Inter-specific variations in distribution, abundance and possible life-cycle patterns of *Themisto* spp. (Amphipoda) in the Barents Sea. *Polar Biology* **25**: 656–666.
- , AND H. R. SKJOLDAL. 1991. Distribution and life history of krill from the Barents Sea. *Polar Research* **10**: 443–460.
- DEINES, K. L. 1999. Backscatter estimation using broadband acoustic Doppler current profilers, p. 249–253. *In Proceedings of the IEEE Sixth Working Conference on Current Measurements*. 4
- DE ROBERTIS, A. 2002. Small-scale spatial distribution of the euphausiid *Euphausia pacifica* and overlap with planktivorous fishes. *J. Plankton Res.* **24**: 1207–1220.
- FALK-PETERSEN, S., T. M. DAHL, C. L. SCOTT, J. R. SARGENT, B. GULLIKSEN, AND R.-M. MILLAR. 2001. Lipid biomarkers and trophic linkages between the arctic ctenophores and calanoid copepods in Svalbard waters. *Mar. Ecol. Prog. Ser.* **277**: 187–194.
- , R. R. GATTEN, J. R. SARGENT, AND C. C. E. HOPKINS. 1981. Ecological investigations on the zooplankton community in Balsfjorden, Northern Norway: Seasonal changes in the lipid class composition of *Meganycitiphanes norvegica* (M.Sars), *Thysanoessa raschii* (M. Sars) and *T. inermis* (Kroyer). *J. Exp. Mar. Biol. Ecol.* **54**: 209–224.
- , AND Å. KRISTIANSEN. 1985. Acoustic assessment of krill stocks in Ullsfjorden, North-Norway. *Sarsia* **70**: 83–90.
- , G. PEDERSEN, S. KWASNIEWSKI, E. N. HEGSETH, AND H. HOP. 1999. Spatial distribution and life-cycle timing of zooplankton in the marginal ice zone of the Barents Sea during the summer melt season in 1995. *J. Plankton Res.* **21**: 1249–1264.
- FIKSEN, O., AND F. CARLOTTI. 1998. A model of optimal life-history and diel vertical migration in *Calanus finmarchicus*. *Sarsia* **83**: 129–147.
- FISCHER, J., AND M. VISBECK. 1993. Seasonal variation of the daily zooplankton migration in the Greenland Sea. *Deep-Sea Res. I* **40**: 1547–1557.
- FORTIER, M., L. FORTIER, H. HATTORI, H. SAITO, AND L. LEGENDRE. 2001. Visual predators and the diel vertical migration of copepods under arctic sea ice during the midnight sun. *J. Plankton Res.* **23**: 1263–1278.
- FRANK, T. M., AND E. A. WIDDER. 1997. The correlation of downwelling irradiance and staggered vertical migration patterns of zooplankton in Wilkinson Basin, Gulf of Maine. *J. Plankton Res.* **19**: 1975–1991.
- GAULD, D. T. 1953. Diurnal variation in the grazing of planktonic copepods. *J. Mar. Biol. Assoc. UK* **31**: 461–474.

- GLIWICZ, Z. M. 1986. Predation and the evolution of vertical migration behaviour in zooplankton. *Nature* **320**: 746–748.
- GREENE, C. H., P. H. WIEBE, A. J. PERSHING, G. GAL, J. M. POPP, N. J. COPLEY, T. AUSTIN, A. M. BRADLEY, R. G. GOLDSBOROUGH, J. DAWSON, R. HENDERSHOTT, AND S. KAARTVEDT. 1998. Assessing the distribution and abundance of zooplankton: A comparison of acoustic and net-sampling methods with D-BAD MOCNESS. *Deep-Sea Res. II* **45**: 1219–1237.
- HAYS, G. C., H. KENNEDY, AND B. W. FROST. 2001. Individual variability in diel vertical migration of a marine copepod: Why some individuals remain at depth when others migrate. *Limnol. Oceanogr.* **46**: 2050–2054.
- HEYWOOD, K. J. 1996. Diel vertical migration of zooplankton in the Northeast Atlantic. *J. Plankton Res.* **18**: 163–184.
- HOP, H., T. PEARSON, E. N. HEGSETH, K. M. KOVACS, C. WIENCKE, S. KWASNIEWSKI, K. EIANE, F. MEHLUM, B. GULLIKSEN, M. WŁODARSKA-KOWALCZUK, C. LYDERSEN, J. M. WESLAWSKI, S. COCHRANE, G. W. GABRIELSEN, R. J. G. LEAKEY, O. J. LØNNE, M. ZAJACZKOWSKI, S. FALK-PETERSEN, M. KENDALL, S.-A. WÄNGBERG, K. BISCHOF, A. Y. VORONKOV, N. A. KOVALTCHOUK, J. WIKTOR, M. POLTERMANN, G. DI PRISCO, C. PAPUCCI, AND S. GERLAND. 2002. The marine ecosystem of Kongsfjorden, Svalbard. *Polar Research* **21**: 167–208.
- KILS, U. 1981. Swimming behaviour, swimming performance and energy balance of Antarctic krill *Euphausia superba*, p. 1–121. *BIOMASS Scientific Series*.
- [5] KWASNIEWSKI, S., H. HOP, S. FALK-PETERSEN, AND G. PEDERSEN. 2003. Distribution of *Calanus* species in Kongsfjorden, a glacial fjord in Svalbard. *J. Plankton Res.* **25**: 1–20.
- MACKAS, D., AND R. BOHRER. 1976. Fluorescence analysis of zooplankton gut contents and an investigation of diel feeding patterns. *J. Exp. Mar. Biol. Ecol.* **25**: 77–85.
- MARSHALL, S. M., AND A. P. ORR. 1955. The biology of a marine copepod *Calanus finmarchicus* (Gunnerus). Oliver and Boyd.
- MAUCHLINE, J. 1998. The biology of calanoid copepods. *Adv. Mar. Biol.* **33**: 1–710.
- MINKINA, N. I. 1981. Estimation by hydrodynamic method of energy expenditure of copepods (Copepoda, Crustacea) on swimming. *Doklady Akad. Nauk SSSR Biol. Sci.* **257**: 141–144.
- PEARRE, S. 1970. Light responses and feeding behaviour of *Sagitta elegans*. Ph.D. thesis, Dalhousie Univ.
- . 1973. Vertical migration and feeding in *Sagitta elegans* (Verrill). *Ecology* **54**: 300–314.
- . Problems of detection and interpretation of vertical migration. *J. Plankton Res.* **1**: 20–44.
- . 2003. Eat and run? The hunger/satiation hypothesis in vertical migration: History, evidence and consequences. *Biol. Rev.* **78**: 1–79.
- PLUEDDEMANN, A. J., AND R. PINKEL. 1989. Characterization of the patterns of diel migration using a Doppler sonar. *Deep-Sea Res.* **36**: 509–530.
- RINGELBERG, J. 1995. Changes in light intensity and diel vertical migration—a comparison of marine and fresh-water environments. *J. Mar. Biol. Assoc. UK* **75**: 15–25.
- ROE, H. S. J. 1983. Vertical distributions of euphausiids and fish in relation to light-intensity in the Northeastern Atlantic. *Mar. Biol.* **77**: 287–298.
- SCOTT, C. L., S. KWASNIEWSKI, S. FALK-PETERSEN, R.-M. MILLAR, AND J. R. SARGENT. 2000. Life strategy of arctic copepods: Stage distribution and lipids of *Calanus finmarchicus*, *Calanus glacialis* and *Calanus hyperboreus* in late autumn, Kongsfjord, Svalbard. *Polar Biol.* **23**: 510–516.
- SIMARD, Y., G. LACROIX, AND L. LEGENDRE. 1985. *In situ* twilight grazing rhythm during diel vertical migrations of a scattering layer of *Calanus finmarchicus*. *Limnol. Oceanogr.* **30**: 598–606.
- , R. D. LADURANTAYE, AND J. C. THERRIAULT. 1986. Aggregation of euphausiids along a coastal shelf in an upwelling environment. *Mar. Ecol. Prog. Ser.* **32**: 203–215.
- STANTON, T. K., P. H. WIEBE, D. CHU, M. C. BENFIELD, L. SCANLON, L. MARTIN, AND R. L. EASTWOOD. 1994. On acoustic estimate of zooplankton biomass. *ICES J. Mar. Sci.* **51**: 505–512.
- SVENDSEN, H., A. BESZCZYNSKA-MØLLER, J. O. HAGEN, B. LEFAUCONNIER, V. TVERBERG, S. GERLAND, J. B. ØRBÆK, K. BISCHOF, C. PAPUCCI, M. ZAJACZKOWSKI, R. AZZOLINI, O. BRULAND, C. WIENCKE, J.-G. WINTHER, AND W. DALLMANN. 2002. The physical environment of Kongsfjorden–Krossfjorden, an arctic fjord system in Svalbard. *Polar Res.* **21**: 133–166.
- TARLING, G. A., J. B. L. MATTHEWS, P. DAVID, O. GUERIN, AND F. BUCHHOLZ. 2001. The swarm dynamics of northern krill (*Meganctipanes norvegica*) and pteropods (*Cavolinia inflexa*) during vertical migration in the Ligurian Sea observed by an acoustic Doppler current profiler. *Deep-Sea Res. I* **48**: 1671–1686.
- , T. JARVIS, S. M. EMSLEY, AND J. B. L. MATTHEWS. 2002. Midnight sinking behaviour in *Calanus finmarchicus*: A response to satiation or krill predation? *Mar. Ecol. Prog. Ser.* **240**: 183–194.
- WESLAWSKI, J. M., G. PEDERSEN, S. FALK-PETERSEN, AND K. PORAZINSKI. 2000. Entrapment of macrozooplankton in an arctic fjord basin, Kongsfjorden, Svalbard. *Oceanol. Acta* **47**: 109–114.
- WIDDER, E. A., AND T. M. FRANK. 2001. The speed of an isolume: A shrimp's eye view. *Mar. Biol.* **138**: 669–677.
- WIEBE, P. H., S. H. BOYD, B. M. DAVIS, AND J. L. COX. 1982. Avoidance of towed nets by the euphausiid *Nematoscelis megalops*. *Fish. Bull.* **80**: 75–91.
- , N. J. COPLEY, AND S. H. BOYD. 1992. Coarse-scale horizontal patchiness and vertical migration of zooplankton in Gulf Stream warm-core ring 82-H. *Deep-Sea Res.* **39**: S247–S278.
- WILLIS, K. J., F. R. COTTIER, S. KWASNIEWSKI, A. WOLD, AND S. FALK-PETERSEN. In press. The influence of advection on zooplankton community composition in an arctic fjord (Kongsfjorden, Svalbard). *J. Mar. Syst.* [6]

Received: 19 August 2005

Accepted: 30 April 2006

Amended: 1 June 2006

*Authors Queries*Journal: **Limnology**Paper: **limn-51-06-04**Title: **Unsynchronized and synchronized vertical migration of zooplankton in a high arctic fjord**

Dear Author

During the preparation of your manuscript for publication, the questions listed below have arisen. Please attend to these matters and return this form with your proof. Many thanks for your assistance

Query Reference	Query	Remarks
1	Author: This article has been lightly edited for grammar, style, and usage. Please compare it with your original document and make corrections on these pages. Please limit your corrections to substantive changes that affect meaning. If no change is required in response to a question, please write "OK as set" in the margin. Copy editor	
2	Author: In paragraph beginning, "An average L for Calanus," please define stages CV, CIV, and CIII, if appropriate (and also in Table 1).	
3	Author: Please approve insertion of in-text callout for Fig. 9 (in sentence beginning, "A synthesis of the surface irradiance data"). If it is incorrectly placed, please indicate correct placement in order.	
4	Author: Deines 1999: Please provide page range; names of editors, if relevant; and name of publisher or sponsoring body.	
5	Author: Kils 1981: Please clarify entry: Is this an article in a book, or is it part of a monograph series?	
6	Author: Willis et al. in press: Please update if possible with year, volume, page range. Please update in text too as needed.	